Mircophysical peoperties of cirrus cloud praticles as derivied from CloudSat/CALIPSO

Eyk Boesche, D.P. Donovan, and Gerd-Jan van Zadelhoff

KNMI, PO Box 201, 3730 AE, the Netherlands, donovan@knmi.nl

ABSTRACT

Through their interaction with solar and thermal radiation, ice clouds are important in determining atmospheric and surface heating rates. To derive microphysical properties of ice clouds, we adapted a combined radar and lidar approach for ground-based measurements, developed at the KNMI, to data from CloudSat and CALIPSO. To validate the KNMI Lidar/Radar algorithm we performed an error assessment/sensitivity study using synthetic data.

The ultimate aim of this study is to develop an ice cloud effective size parameterization suitable for application in climate and forecast models. An earlier study, using geographically limited ground-based lidar and radar measurements, revealed certain limitations of attempting to parameterize the global description of ice cloud particle size (R_{eff}) as a function of temperature (T) and ice water content (IWC) and showed a possible solution by describing R_{eff} as a function of normalized depth into cloud $R_{eff}(\Delta Z/H)$. Using CloudSat and CALIPSO data the retrieved microphysical properties of ice clouds at high-, mid- and low-latitudes have been analyzed. The effective particle size and ice water content were derived and correlated to temperature and depth into the cloud from cloud top. It is shown that the relation between R_{eff} and $\Delta Z/H$, for different classes of total cloud thicknesses (H), allows for a single parameterization valid in all three latitude regimes.

1. INTRODUCTION

This study builds upon the earlier work described in [2, 1] in which a large amount of ground-based combined lidar and radar measurements of ice cloud effective radius (R_{eff}) and Ice water content IWC were derived and analyzed. This work has extended the original lidar+radar method developed by [3] to be applicable to the CloudSat/CALIPSO combination.

Section 2 of this paper describes the retrieval approach while Section 3 describes the observed relationships between temperature, cloud depth and R_{eff}.

2. RETRIEVAL PROCEDURE

The procedure described earlier in [3] is best suited for application to IR wavelengths. In this work the 532 nm channel of CALIPSO is used so an alternate procedure has been developed.

The lidar signal for a CALIPSO-type instrument can be written as:

$$\begin{aligned} p(z) &= \frac{C_{lid}}{(z_{lid}-z)^2}\left(\beta_R(z)Ms_R^{-1}(z)+\beta_M Ms_M^{-1}(z)\right) \\ &\times \quad e^{-2\int_0^z\left(\alpha_M(z')+\alpha_R(z')\right)dz'} \end{aligned} \tag{1}$$

where C_{lid} is the lidar calibration constant, β denotes backscatter ,α denotes extinction while the R subscript indicates Rayleigh and M indicates Mie (or generally cloud/aerosol) backscatter or extinction, z is the altitude coordinate, z_{lid} is the lidar altitude and $Ms(z)$ is the altitude dependent multiple scattering factor (which may, in general, be different for both the Rayleigh and Mie signals).

If we define:

$$P(z) \equiv Ms(z)(z_{lid}-z)^2 p(z) S(z) e^{2\int_0^2 \alpha_R(z')+2S\beta_M(z')dz'} \tag{2}$$

where we have assumed $Ms_R(z) = Ms_M$ and $S = \frac{\alpha(z)}{\beta(z)}$ is assumed to be constant with altitude, then Eqn. (1) can be written as

$$P(z) = C\left(\alpha(z)+S\beta_R(z)\right)\exp[-2\tau'(z_{lid},z)] \tag{3}$$

where $\tau'(z_1,z) = \int_{z_1}^{z}\left(\alpha_M(z')+S\beta_M(z')\right)dz$. Eqn. (3) is a differential equation whose solution in terms of α can be written as

$$\alpha(z) = -\frac{1}{2}\left[\frac{P(z)}{\frac{P(z_o)}{\alpha_o - S\beta_R} - 2\int_{z_o}^{z}P(z')dz'}\right] - S\beta_R(z) \tag{4}$$

Where α_o is the lidar extinction coefficient at some boundary range z_o. Once the extinction profile has been determined, the lidar-radar effective radius (R'_{eff}) profile and the effective radius (R_{eff}) and IWC profiles are determined assuming a crystal habit model following an approach similar to that in [3].

In order to account for the unknown parameters in Eqn.(4) the following procedure is used.

1– z_o is chosen at the range furthest from the lidar where both the Lidar and Radar both detect cloud and the estimated SNR is above 2-3.

© Proceedings of the 8th International Symposium on Tropospheric Profiling, ISBN 978-90-6960-233-2
Delft, The Netherlands, October 2009. Editors, A. Apituley, H.W.J. Russchenberg, W.A.A. Monna

2– Eqn.(4) is solved by first setting $Ms(z) = 1$ and treating S and α_o as free parameters and choosing those that minimize the following cost function

$$C_f(S,\alpha_o) = \sum_{i=nocld} \left(\frac{R_i - 1.0}{\delta R}\right)^2 + \left(\frac{S - S_a}{\delta S_a}\right)^2 + \gamma \sum_{i:i_o<i<i_o-4} \left(\frac{R'_{eff,i} - R'_{eff,i+1}}{R'_{eff,i}}\right)^2 \quad (5)$$

where S_a is the a priori estimate of S with associated uncertainty δS_a, R is the backscatter ratio ($R = 1.0 + \beta_M/\beta_R$) and γ is a Lagrange multiplier chosen on the basis of simulations. The first term in Eqn. 5 attempts to force the retrieved R to 1 where no cloud is assumed. The second term constrains the S ratio to a reasonable range while the third term nudges the retrieval towards the smoothest effective particle size profile. In conditions where useful cloud free signal exists below the cloud then the influence of the 3rd term is small but increases in importance when the cloud is thicker and cloud-free returns below the cloud are not present.

The minimization is performed using a simplex algorithm and is carried out using the logarithm of the control variables in order to enforce positivity.

3– The effective particle size profile and the extinction profile together with a multiple-scattering model [4, 5] is used to estimate the $Ms(z)$ profile. The procedure then returns to Step 2 and loops until the retrieved profile converges.

2.1. Simulations

The retrieval procedure was applied to a number of representative scenarios using CloudSat and CALPSIO simulated data generated using the EarthCARE simulator (For more information on ECSIM please see the ECSIM Models and Algorithms Document (`ECSIM_MAD.pdf`) which can be downloaded from `ftp:bbc.knmi.nl,user:simguest, Password:S139st, Directory:ECSIMV1P3`). The ECSIM "scenes" were generated based on the same in-situ data set used in [6].

The cost-function (Eq.(5) as a function of S and α_o is shown for 2 synthetic cases in Fig. 1. The cases shown here illustrate that reliable results can be obtained for both thin clouds as well as optically thick clouds. In optically thick cases points past the normalization range usually have a high associated error and are thus discarded.

3. APPLICATION TO DATA

An example application of the algorithm to CloudSAT and CALIPSO data is shown in Fig. 2. In this example it can be seen that the estimated effective radii are mainly in the 30 micron region and generally increase with depth into the cloud.

The relationship between R_{eff} and Temperature as well as R_{eff} and depth into cloud for 1-month of data is shown in Figs. 3 and 4. The data has been separated into observations made between -20 and +20 Deg of Latitude and observations made at Mid-latitudes. The results of the preliminary data analysis seem consistent with the previous ground-based results shown in [1]. In particular, the relationship between R_{eff} and normalized cloud depth seems less geographically dependent than the relationship between R_{eff} and Temperature.

4. SUMMARY

We retrieved microphysical properties of ice clouds at high-, mid- and low-latitudes from CloudSat/CALIPSO measurements. The effective particle size and ice water content were derived and correlated to temperature and depth into cloud from cloud top (ΔZ/H). It is shown that the relation of R_{eff} to $\Delta Z/H$, for different classes of total cloud thicknesses (H), may allow for a single parameterization valid in all three latitude regimes. This preliminary study has to be extended to a larger dataset and investigation of land-ocean relations, to verify the correctness of the approach.

ACKNOWLEDGMENTS

This work was carried out as part of SRON project EO-083 . We also would like to thank J. Delano for supplying the co-located CloudSat and CALIPSO data used and Robin Hogan for supplying the in situ derived data sets used to construct the ECSIM scenes.

REFERENCES

[1] van Zadelhoff G-J, E. van Meijgaard, R. Boers, D.P. Donovan, W. Knap, 2007: Sensitivity of the shortwave radiative budget to the parameterization of ice crystal effective radius,*J. Geophys. Res.*,**112**, doi:10.1029/2006JD007791.

[2] Donovan, D. P., and A. C. A. P. van Lammeren, 2002: First ice cloud effective particle size parameterization based on combined lidar and radar data, *Geophys. Res. Lett.*, **29**, doi:10.1029/2001GL013731.

[3] Donovan, D.P., A.C.A.P. van Lammeren, 2001: Cloud effective particle size water content profile retrievals using combined lidar and radar observations. Part I: Theory and simulations. *J. Geophys. Res* **21**, 27,425-27,445.

[4] Hogan, R., 2006: Fast approximate calculation of multiply scattered lidar returns. *Appl. Opts.*, **45**, 5984–5992.

[5] Eloranta, E., 1998: Practical model for the calculation of multiply scattered lidar returns. *Appl. Opts.*, **37**, 2464–2472.

[6] Hogan, R. J., D. P. Donovan, C. Tinel, M. A. Brooks, A. J. Illingworth and J. P. V. Poiares Baptista. 2006: Independent evaluation of the ability of spaceborne radar and lidar to retrieve the microphysical and radiative properties of ice clouds *J. Atmos. Oceanic Technol.*, **23**, 211-227.

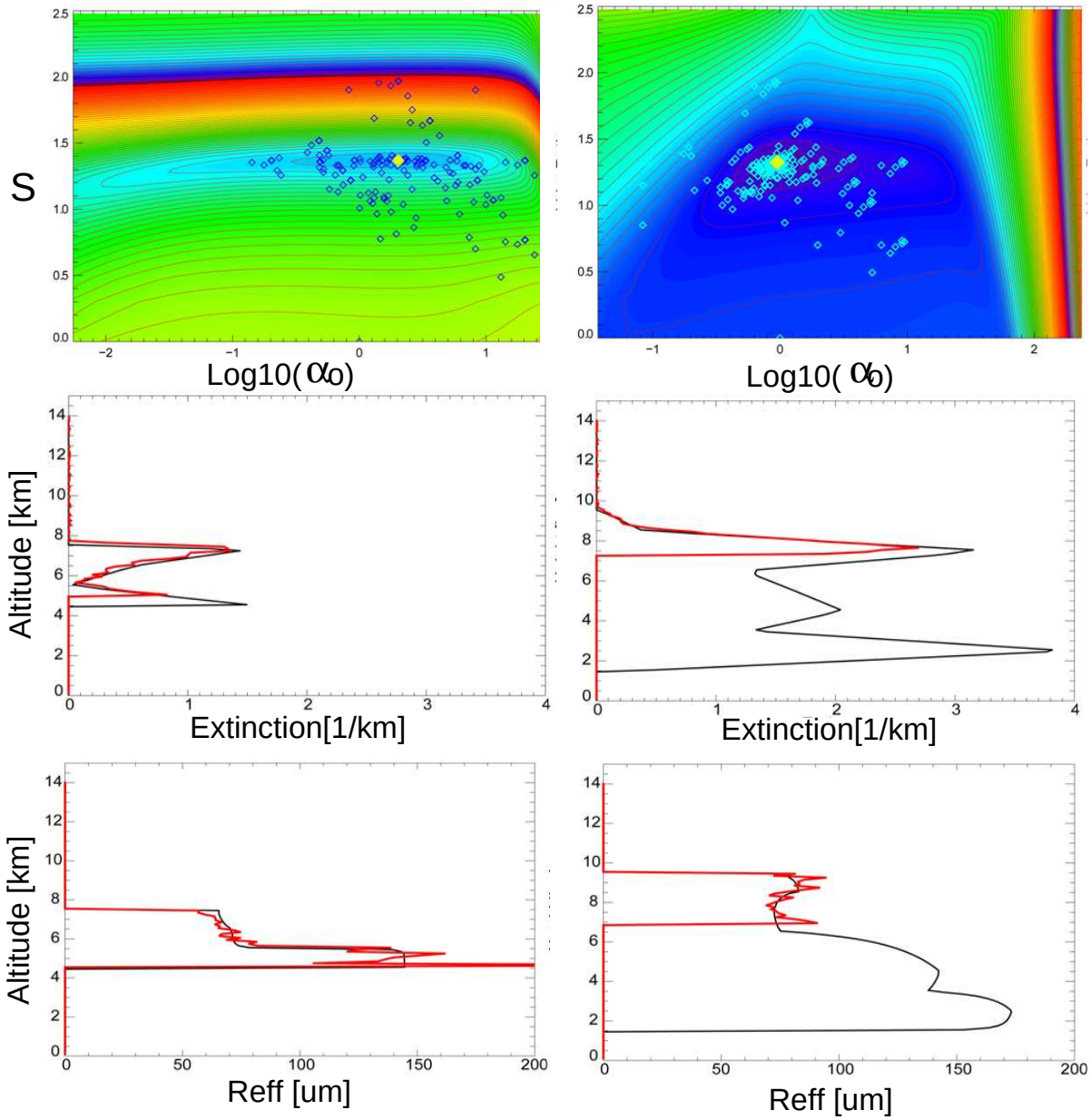

Figure 1. ***(Top panel) (left):*** *Thin cloud with an optical thickness of 2.* ***(right):*** *Thick cloud with an optical thickness of 14. The yellow diamond denotes the optimum fit found by the minimization routine, while the blue diamonds denote intermediate steps.* ***(Middle panel):*** *Extinction as a function of height. The black lines show the test case "truth" and the red lines the results derived by using the Lidar/Radar algorithm.* ***(Lower panel):*** *Effective radius as a function of height. The black lines show the test case "truth" and the red lines the results derived by using the Lidar/Radar algorithm.*

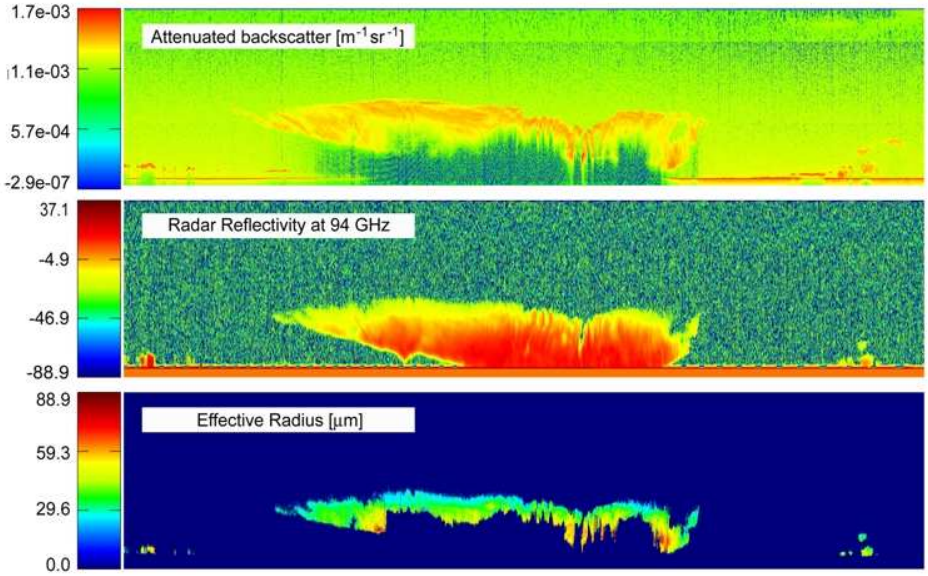

Figure 2. Microphysical properties of ice clouds as derived from CloudSat/CALIPSO measurements for June 21, 2006. ***(top panel):*** *CALIPSO/Lidar - attenuated backscatter signal.* ***(middle panel):****CloudSat/Radar - 94 GHz radar reflectivity.* ***(bottom panel):*** *Derived effective radius. Here the altitude goes from the ground to 30 km.*

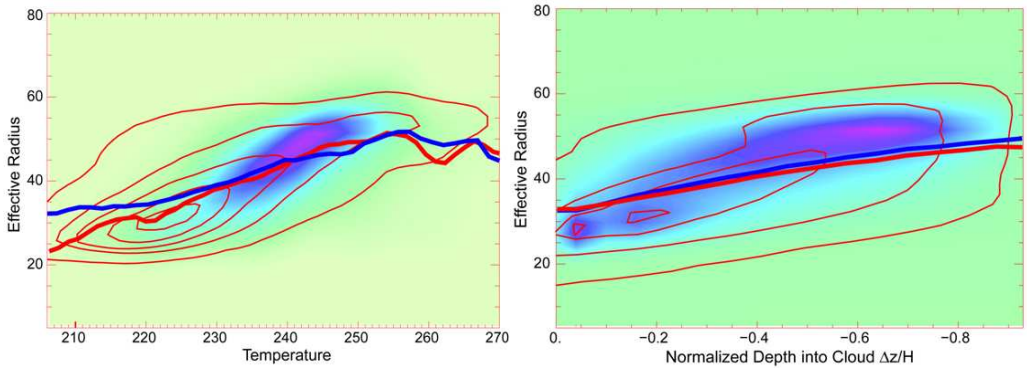

Figure 3. Cumulative probability of occurrence of the effective radius as function of temperature ***(left)*** *and normalized depth into cloud* ***(right)*** *for data observed above(below) 20(-20) degrees of latitude. The thick blue line gives the corresponding mean particle size. The contour lines depict the probability occurrence for data observed between 20 and -20 degree latitude. The thick red line gives the corresponding mean particle size.*

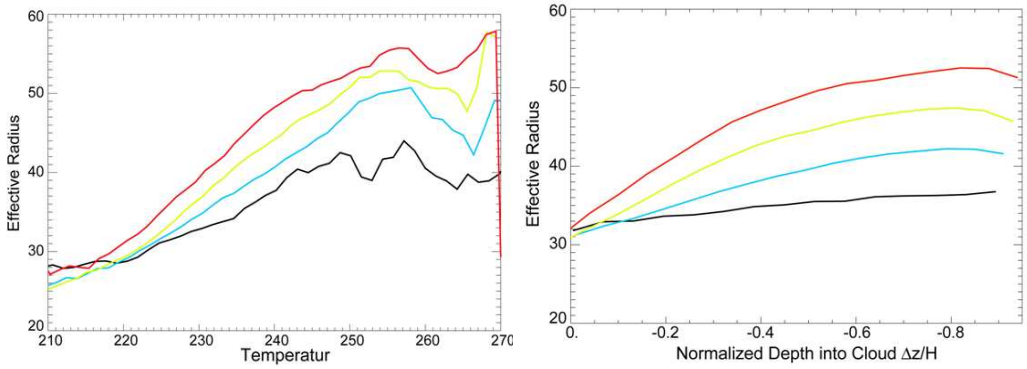

Figure 4. Effective Radius as a function of temperature ***(left)*** *and normalized depth into cloud* ***(right)****, seen from cloud top, for four different total geometrical cloud thickness [H(km)] regimes (H>4.5 (red); 3.0<H<4.5 (yellow);1.5<H<3.0 (blue); and H<1.5 (black)), for data observed above 20 degree latitude. Note that the cloud top is at 0 and cloud bottom at -1.*